frontiers | Frontiers in Marine Science

TYPE Original Research
PUBLISHED 11 December 2023
DOI 10.3389/fmars.2023.1204992

OPEN ACCESS

EDITED BY
Elva G. Escobar-Briones,
National Autonomous University of Mexico, Mexico

REVIEWED BY
Wang Minxiao,
Chinese Academy of Sciences (CAS), China
Hilary G. Close,
University of Miami, United States

*CORRESPONDENCE
Kyung-Hoon Shin
shinkh@hanyang.ac.kr

RECEIVED 13 April 2023
ACCEPTED 27 November 2023
PUBLISHED 11 December 2023

CITATION
Suh YJ, Ju S-J, Kim M-S, Choi H and Shin K-H (2023) Trophic diversity of chemosymbiont hosts in deep-sea hydrothermal vents using amino acid nitrogen isotopes.
Front. Mar. Sci. 10:1204992.
doi: 10.3389/fmars.2023.1204992

Trophic diversity of chemosymbiont hosts in deep-sea hydrothermal vents using amino acid nitrogen isotopes

Yeon Jee Suh[1], Se-Jong Ju[1], Min-Seob Kim[2], Hyuntae Choi[3] and Kyung-Hoon Shin[3]*

[1]Global Georesources Research Department, Korea Institute of Ocean Science and Technology, Busan, Republic of Korea, [2]Environmental Measurement and Analysis Center, National Institute of Environmental Research, Incheon, Republic of Korea, [3]Department of Marine Sciences and Convergent Technology, College of Science and Technology, Hanyang University, Ansan, Republic of Korea

Chemosymbiotic species inhabiting deep-sea hydrothermal vents are known to rely on microbial symbionts for nutrition. However, the relative contributions of heterotrophic energy sources to their diets remain poorly understood. In this study, we investigate the trophic positions (TP) of symbiont-bearing taxa, including vent mussels, snails, and shrimps, and examine the contribution of copepods and detrital organic matter (OM) to the food chain. Amino acid nitrogen isotopic compositions ($\delta^{15}N_{AA}$) were used to investigate the TP of vent mussels (*Bathymodiolus septemdierum* and *Gigantidas vrijenhoeki*), snails (*Alviniconcha* spp.), and shrimps (*Alvinocaris* sp. and *Rimicaris kairei*) from two different vent environments. $\delta^{15}N_{AA}$ values in copepods and OM were also measured. Microbial resynthesis index (ΣV) was calculated to predict the contribution of reworked OM as an energy source to the hydrothermal vent ecosystem. Variations in TP were observed among vent mussels and snails from different vent environments, with higher TP in species from diffusing vents than in those from black smoker vents. Shrimps dwelling in a single diffusing vent exhibited distinct TP, suggesting that microhabitat and phylogeny may influence their energy acquisition. Notably, copepods occupied higher TPs than expected, possibly owing to the consumption of detrital OM. Our findings provide new insights into the trophic diversity of chemosymbiotic species in deep-sea hydrothermal vents and demonstrate the utility of $\delta^{15}N_{AA}$ analysis as a tool for unraveling food web dynamics and ecosystem functioning in these unique environments.

KEYWORDS

food web, trophic position, compound-specific amino acid analysis, $\delta^{15}N$, chemosynthesis, diet source, heterotrophic source

1 Introduction

The discovery of lightless ecosystems in hydrothermal vents in the Galapagos Ridge in 1977 revolutionized our understanding of primary production on Earth (Lonsdale, 1977; Corliss et al., 1979; Jannasch and Wirsen, 1979; Fisher et al., 1988; Childress and Fisher, 1992). A notable feature of these ecosystems is the symbiotic partnership between chemosynthetic bacteria and their eukaryotic hosts (Childress and Fisher, 1992). Vent microbes, including both free-living and symbiotic bacteria, fix CO_2 using the energy produced during the redox reaction of inorganic substrates, such as sulfide or methane from vents (Rau and Hedges, 1979; Rau, 1981a). Host animals harvest symbionts with the advantage of gaining access to energy sources that they cannot use directly; however, the relative contribution of heterotrophic energy sources and nutrients consumed by hosts to meet their nutritional demands remains unknown.

Understanding the nutritional relationship between symbiotic bacteria and host animals is critical for comprehending the energy flow and community structure of hydrothermal vent ecosystems. Prior studies utilized stable isotopic compositions, fatty acids, stomach content analysis, and observations to unravel nutritional sources and trophic relations in vent fauna (Kennicutt et al., 1992; Fisher et al., 1994; Pond et al., 1997; Polz et al., 1998; Colaço et al., 2002; Naraoka et al., 2008; Erickson et al., 2009; Wang et al., 2018; Salcedo et al., 2021; Suh et al., 2022a). Among these methods, bulk carbon ($\delta^{15}C_{bulk}$) and nitrogen isotope ($\delta^{15}N_{bulk}$) values have been extensively utilized in investigating vent food webs (Fisher et al., 1994; Colaço et al., 2002; Suh et al., 2022a). These methods offer the advantage of elucidating diet compositions over preceding weeks or months. Isotopic signatures demonstrate a consistent fractionation of approximately 1‰ for carbon and 3-4‰ for nitrogen between prey and predator, thereby enabling the interpretation of prey-predator relationships (Post 2002).

However, $\delta^{15}C_{bulk}$ and $\delta^{15}N_{bulk}$ values are not exclusively sensitive to TP; they are also influenced by the energy source and metabolic pathways of organisms. Although the isotope fractionation in $\delta^{15}C_{bulk}$ values in vent fauna are relatively well known, the factors that affect $\delta^{15}N_{bulk}$ values are poorly understood. Vents have both, inorganic (NH_4^+, NO_3^-, NO_2^-, and N_2) and organic nitrogen (dissolved organic nitrogen and amino acids) sources (Bourbonnais et al., 2012), which may have distinct $\delta^{15}N_{bulk}$ values and isotope fractionation during nitrogen cycling (Bourbonnais et al., 2012; Charoenpong, 2019). For instance, vent fauna that mainly utilize NO_3^- have $\delta^{15}N_{bulk}$ values above 5‰, whereas those that assimilate ammonium have values below 5‰ (Lee and Childress, 1994; Bourbonnais et al., 2012). Furthermore, N_2 fixation has been reported to reduce $\delta^{15}N$ values (Fry, 2006), and ammonium assimilation can cause fractionation up to 20-30‰ depending on the NH_4^+ concentration (Bourbonnais et al., 2012; Portail et al., 2018), although *in situ* quantification is yet to be established. The presence of various nitrogen sources utilized by vent fauna, coupled with the uncertainty in $\delta^{15}N$ values, poses a challenge when using $\delta^{15}N_{bulk}$ values to accurately estimate their TP. If the TP of basal consumers is not accurately established, the entire food web structure may be poorly understood.

For example, $\delta^{15}N_{bulk}$ values of vent mussels exhibit variability across mussel populations among distinct vent sites (Colaço et al., 2002; Naraoka et al., 2008; Van Audenhaege et al., 2019). It is challenging to determine whether such fluctuations arise from variation in source $\delta^{15}N$ values or TP solely based on $\delta^{15}N_{bulk}$ values. To address this, Vokhshoori et al. (2021) employed amino acid nitrogen stable isotope ($\delta^{15}N_{AA}$) analysis to unravel dietary characteristics of a mussel (*B. childressi*) from seep sites located at water depths of 390-1490m. This investigation revealed that *B. childressi* exhibits mixotrophic behavior, with the contribution of heterotrophic sources linked to venting intensity and mussel bed size. Similarly, *Alviniconcha* snails also harvest symbiotic bacteria from their gill tissues and are often categorized as primary consumers (Suzuki et al., 2005a; Suzuki et al., 2005b; Suzuki et al., 2006). While several studies reported carbon fixation pathways of *Alviniconcha* snails' symbionts (Suh et al., 2022b; Jang et al., 2023), investigation of the precise TP of the host snail remains limited.

In this study, the TP of ecologically important and symbiont-bearing vent species, such as vent mussels (*Bathymodiolus septemdierum* and *Gigantidas vrijenhoeki*), hairy snails (*Alviniconcha* spp.), and shrimps (*Rimicaris kairei* and *Alvinocaris* sp.), were estimated using $\delta^{15}N_{AA}$. The advantage of $\delta^{15}N_{AA}$ analyses is that they provide TPs for organisms, from primary producers to top predators, without requiring source nitrogen $\delta^{15}N$ values (Chikaraishi et al., 2009; McMahon and McCarthy, 2016; Ohkouchi et al., 2017). This study also compared congeners collected from two ecologically different vent sites (a diffusive vent in the Central Indian Ridge and a black smoker vent from the North Fiji Basin, Southwest Pacific) to investigate environmental impacts on TP and reveal phylogenetic variation in the TP of shrimps within a single vent site. Additionally, detritus and copepod spp. were collected and analyzed for $\delta^{15}N_{AA}$ values to examine their contribution to the macrofaunal community as possible energy sources.

Microbes play crucial roles in energy production and decomposition in vents. To understand the consumption of microbially resynthesized energy by host taxa, the study calculated $\delta^{15}N_{AA}$ based ΣV parameter, a proxy for total heterotrophic resynthesis proposed by McCarthy et al. (2007). If symbiont hosts consume microbially resynthesized energy in addition to the energy newly synthesized by symbionts, this suggests that they play a dual role as primary consumers and detritivores, contributing to vent energy recycling. The use of $\delta^{15}N_{AA}$ values as an indicator of chemosynthetic sources and mechanisms of nitrogen utilization has been proven in cold seeps (Vokhshoori et al., 2021; Wang et al., 2022) and shallow water hydrothermal vents (depth > 30m) (Chang et al., 2018), This study is the first to explore TP in deep-sea (> 2,000 m) hydrothermal vents with no or negligible contribution of photosynthetic OM. We believe that this study contributes to improving the interpretation of $\delta^{15}N_{AA}$ values to better understand the function and energetics of deep-sea hydrothermal vent ecosystems.

2 Materials and methods

2.1 Study site and sample collection

The Onnuri Vent Field (OVF; 11°24.9′ S, 66°25.4′ E) is a diffusive vent located in the Central Indian Ridge characterized by

high biological density, high concentrations of dissolved methane, and a lack of plume particles (Kim et al., 2020; Suh et al., 2022b). During the KIOST Indian Ocean cruise conducted in June 2018 using R/V Isabu, megafaunal samples were collected from the OVF using a video-guided hydraulic grab (Oktopus, Germany). This study focused on analyzing a few symbiont-bearing endemic vent fauna species, including two mussel species (*Gigantidas vrijenhoeki* and *Bathymodiolus septemdierum*), a hairy snail (*Alviniconcha marisindica*), and two shrimp species (*Rimicaris kairei* and *Alvinocaris* sp.). In November 2021, the OVF was revisited using a remotely operated platform for ocean science (ROPOS) to collect samples of possible dietary sources of megafauna by suctioning settled particles and OM in and around the biological community. The copepod *Stygiopontius spinifer* (Lee et al., 2020) was manually isolated from the suctioned sample, and the remaining suctioned sample was size-fractioned using nested sieves of 100 µm and 38 µm mesh. The particles with a size between 38 and 100 µm were transferred to pre-ashed (450°C, for 5h) glass jars and the remaining particles smaller than 38µm size (detritus hereafter) was filtered using pre-ashed (450°C, for 5h) 47 mm GF/F. Bacterial mats on the outer shells of the mussel *B. septemdierum* were collected separately and stored in pre-ashed (45°C, for 5h) glass vials. All samples were stored at -80°C until analysis.

Mussels (*B. septemdierum*) and snails (*Alviniconcha boucheti*) were collected from an active black smoker chimney (R1964; 18° 51′ S, 173° 29′ E) located in the North Fiji Basin (NFB) to compare their trophic niches with congeners from the OVF diffusing vent. Samples were collected using ROPOS ROV during the KIOST expedition cruise in November and December 2016. Additionally, the copepod *Isaacsicalanus paucisetus* was sampled using a suction sampler of the ROPOS ROV from a diffusing vent (R1971; 16° 59′ S, 173° 55′ E) in the NFB (Park et al., 2020). Megafaunal density was higher in the diffusing vents (OVF and R1971) than in the active black smoker vent (R1964) based on the ROV video camera observation. Upon collection, megafauna samples were frozen at – 80°C and copepods were preserved in 4% formalin. Unfortunately, there were no frozen samples of copepod or settled particulate OM from the NFB for bulk isotope analyses.

2.2 Bulk stable isotope analysis

We compared the stable isotopic compositions of carbon ($\delta^{13}C$) and nitrogen ($\delta^{15}N$) between the gill and muscle tissues of mollusks collected from the NFB, specifically *B. septemdierum* and *A. boucheti*. The isotopic values for the gill and muscle tissues of mollusks from OVF have already been reported in Suh et al. (2022b). The tissues were freeze-dried (FD8518, Ilshin Lab Co., Ltd., Korea) at – 80°C and 5 mTorr for 72 h and homogenized. Subsequently, the samples were treated with a mixture of dichloromethane (DCM): Methanol (MeOH) (2:1, v/v) with sonication to facilitate the lipid removal, following the method described by Bligh and Dyer (1959) with modifications. The copepods (*S. spinifer*) from the OVF was freeze-dried and defatted. Particle samples and bacterial mats from the OVF were freeze-dried and treated with 1N HCl to remove inorganic carbon. Lipid extraction and acid treatment were not performed for $\delta^{15}N$ analysis to prevent treatment effects (Kim et al., 2016). The samples were wrapped in tin capsules for stable isotope analysis.

Stable isotope ratios were determined using an Elemental Analyzer (Vario MicroCube Elementar, Germany) connected to an isotope ratio mass spectrometer (Isoprime Vision Plus, Elementar GV Instrument, Germany). Isotope ratios are reported per mille (‰) using standard delta notation. The carbon and nitrogen references were Vienna PeeDee Belemnite and atmospheric nitrogen (N_2), respectively.

The stable isotope ratios of each element were expressed as values relative to international reference materials as follows (1):

$$\delta^{13}C \ or \ \delta^{15}N \ (‰) = [(R_{sample} / R_{standard} - 1)] \times 1000 \ (‰) \quad (1)$$

Where $R = {}^{13}C/{}^{12}C$ or ${}^{15}N/{}^{14}N$

Reference materials were IAEA-CH-6 (Sucrose, -10.449‰) for ${}^{13}C/{}^{12}C$, and IAEA-N-1 (Ammonium sulfate, 0.4‰) for ${}^{15}N/{}^{14}N$. The analytical precision was within 0.1‰ for C and 0.2‰ for N.

2.3 Nutrient concentration

Water samples were collected from the OVF in June 2022, using Niskin bottles attached to the ROPOS ROV. Water samples were then analyzed for inorganic nitrogen concentrations, including NH_4^+, NO_2^-, and NO_3^-, using a Smart Chem200 nutrient auto-analyzer (Proxima, Alliance Instruments, Italy). The nutrient concentrations in the NFB were previously reported by Suh et al. (2022a).

2.4 Amino acid nitrogen stable isotope analysis

Powdered biota samples were used to measure the nitrogen isotope ratios of individual amino acids (AAs). Each sample (approximately 3 mg) was hydrolyzed for 12-24 h with 6M HCl at 110°C. Subsequently, the hydrophobic content of the samples was removed using 6:5 n-hexane/DCM (v/v). The residual HCl was dried under the flow of N_2 gas at 70°C. Next, AA molecules were derivatized through N-pivaloyl-AA-isopropyl ester using 1:4 thionyl chloride/isopropanol (v/v) at 110°C for 2 h. and 1:4 pivaloyl chloride/DCM (v/v) at 110°C for 2 h in sequence. The AA derivatives were extracted with 6:5 n-hexane/DCM (v/v) to remove the residual hydrophilic content. The AA derivatives were redissolved in DCM and stored in a freezer at -20°C before analysis.

The $\delta^{15}N_{AA}$ values were measured using a gas chromatograph (HP 6890N, Agilent, US) connected to a furnace (GC5 Interface, Elementar, Germany) and an isotope ratio mass spectrometer (Isoprime 100, Elementar, Germany). The analytical precision of $\delta^{15}N$ values was checked every 5–6 runs of samples, using standard mixture of nine AAs, including alanine, glycine, valine, leucine, norleucine, aspartic acid, methionine, glutamic acid, and phenylalanine (SHOKO-Science and Indiana University). During

the analysis, $\delta^{15}N_{AA}$ values of standard mixture showed a standard deviation of less than 1‰.

2.5 Calculation of $\delta^{15}N_{AA}$ parameters

We used the following equations proposed by Chikaraishi et al. (2009) to calculate TP based on $\delta^{15}N$ values of the AAs:

$$TP_{Glu-Phe} = [(\delta^{15}N_{Glu} - \delta^{15}N_{Phe} - \beta_{Glu-Phe}) / TDF_{Glu-Phe}] + 1 \quad (2)$$

$$TP_{Trp-Phe} = [(\delta^{15}N_{Trp} - \delta^{15}N_{Phe} - \beta_{Trp-Phe}) / TDF_{Trp-Phe}] + 1 \quad (3)$$

Where $\delta^{15}N_{Glu}$ and $\delta^{15}N_{Phe}$ are nitrogen isotope values of Glu and Phe, respectively. β denotes the difference in $\delta^{15}N$ values between four trophic AAs and Phe of primary producers, and TDF is the trophic enrichment factor of $\delta^{15}N_{Trp-Phe}$ relative to $\delta^{15}N_{Phe}$ in a trophic transfer. As no isotope fractionation data from chemosynthetic ecosystems were available, we used previously published values of $\beta_{Glu-Phe}$ (3.4‰; Chikaraishi et al., 2009) and $TDF_{Glu-Phe}$ (7.6‰; Vokhshoori et al., 2021). Although the absolute TP values may change slightly, we believe that the interpretation of the overall trend remains unaffected.

For chemosynthetic ecosystem consumers, including this study, Leu and Ile showed low $\delta^{15}N$ values, and Pro exhibited notably high $\delta^{15}N$ values (Vokhshoori et al., 2021), unlike the consumers from photosynthetic ecosystems. Thus, we compared TPs estimated using three different sets of trophic AAs with the $TP_{Glu-Phe}$ values, each employing a varying set of trophic AAs and corresponding $\beta_{Trp-Phe}$ and $TDF_{Trp-Phe}$ values sourced from Chikaraishi et al. (2009): inclusion of (1) all six trophic AAs ($\beta_{Trp-Phe}$ = 3.3‰, $TDF_{Trp-Phe}$ = 5.4‰), (2) Ala, Glu, Val, and Pro ($\beta_{Trp-Phe}$ = 3.6‰, $TDF_{Trp-Phe}$ = 5.9‰), and (3) Ala, Glu, and Val ($\beta_{Trp-Phe}$ = 3.7‰, $TDF_{Trp-Phe}$ = 6.0‰). $\delta^{15}N_{Trp}$ indicates the average nitrogen isotope values of trophic AAs. Moreover, we calculated propagation of errors on TP values using the equation in Jarman et al. (2017).

We also calculated ΣV parameter using six trophic amino acids (Ala, Glu, Ile, Leu, Pro, and Val), as an indication of microbial AA resynthesis, following the equation proposed by McCarthy et al. (2007):

$$\Sigma V = 1/n\Sigma Abs(\chi_{AA}) \quad (4)$$

where χ_{AA} is the deviation of each trophic AA = $\delta^{15}N_{AA}$ - average $\delta^{15}N$ of trophic AAs, and n is the number of trophic AAs used in the calculation. However, variability in ΣV values in hydrothermal vent consumers would vary by characteristic distributions of $\delta^{15}N$ values of trophic AAs (Vokhshoori et al., 2021). Consequently, it becomes challenging to discern whether high ΣV values are a result of microbial resynthesis or species-specific metabolism. We thereby calculated another parameter to evaluate the average isotopic offset in low $\delta^{15}N_{AA}$ values (Leu and Ile) within trophic AAs of hydrothermal vent consumers from the high $\delta^{15}N_{AA}$ (Ala, Val, Pro, and Glu) using the following equation:

$$\text{Leu} - \text{Ile index} = \{(\delta^{15}N_{Ala} + \delta^{15}N_{Val} + \delta^{15}N_{Pro} + \delta^{15}N_{Glu}) / 4\} - \{(\delta^{15}N_{Leu} + \delta^{15}N_{Ile}) / 2\} \quad (5)$$

Among trophic AAs, high $\delta^{15}N_{Pro}$ and low $\delta^{15}N_{Leu}$ and $\delta^{15}N_{Ile}$ values may serve as distinctive $\delta^{15}N$ patterns indicative of methane-oxidizing bacteria, as proposed by Vokhshoori et al. (2021). Thus, we anticipate that a reliance on hydrothermal vent microbes among consumers would be reflected in both ΣV and Leu-Ile index.

2.6 Statistical analysis of variance

The statistical analysis of variance in mean TP of vent fauna was performed using the statistical software package JMP (version 10.0, SAS Institute Inc., Cary, NC, USA). The mean TPs of the three bivalve mussel species were compared using ANOVA ($p< 0.05$) and Tukey-Kramer HSD test ($p< 0.05$; See Supplementary Material), whereas snails, shrimps, and copepods were compared using the *t*-test ($p< 0.05$).

3 Results

3.1 Bulk stable isotopic composition

The muscle $\delta^{15}N$ values of the snail *A. boucheti* and the mussel *B. septemdierum* from the NFB were 11.3 ± 0.2‰ and 10.8 ± 1.9‰, respectively, which are consistently higher than their respective gill $\delta^{15}N$ values by 0.5‰ and 0.4‰ on average (Supplementary Table A1). However, there was no clear pattern observed for $\delta^{13}C$ values between muscle and gill tissues of the gastropods, with differences ranging from -0.06 to 0.7‰.

The detritus (0.7–38 µm) samples (Figure 1A) had a mean $\delta^{13}C$ value of -22.7 ± 0.4‰, but had no detectable $\delta^{15}N$ values (Table 1). Settled particles with a larger size range (38–100 µm) had mean $\delta^{13}C$ value of -17.5 ± 0.0‰, which is ~5‰ higher than detritus (-22.7 ± 0.4‰), with $\delta^{15}N$ value of 2.8 ± 0.0‰. The bacterial mats found on the outer shells of *B. septemdierum* mussels (Figure 1C) had $\delta^{13}C$ and $\delta^{15}N$ values of -27.0‰ and 3.3 ± 0.5‰, respectively. Furthermore, the copepod *S. spinifer* (Figure 1B) had mean $\delta^{15}N$ value of 10.8 ± 0.1‰, which is the highest value among the community members, with also relatively high $\delta^{13}C$ values (-12.8 ± 0.1‰).

3.2 Amino acid nitrogen isotopic composition

The $\delta^{15}N_{AA}$ values for mollusks, shrimps, copepods, and detritus ranged from -14.2‰ to 25.2‰ (Figure 2, Supplementary Table A2). The copepod *I. paucisetus* and shrimp *R. kairei* had only positive $\delta^{15}N_{AA}$ values, with *I. paucisetus* yielding 3.4 to 23.9‰ and *R. kairei* yielding 2.6 to 25.2‰. The mean $\delta^{15}N_{AA}$ values of trophic AAs (Glu, Ala, Ile, Leu, Pro, Val) ranged from -2.1 ± 1.4 ‰ (shrimp *Alvinocaris* sp.) to 18.7 ± 0.5‰ (copepod *I. paucisetus*), having

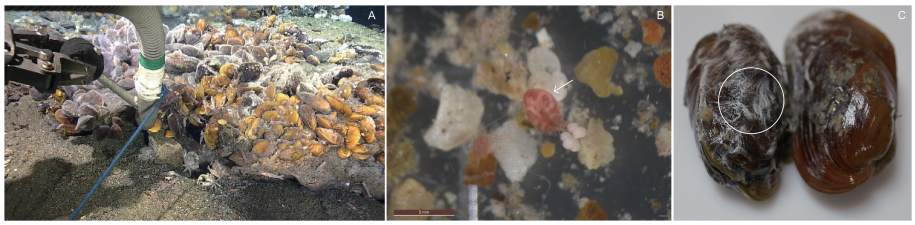

FIGURE 1
(A) Suction sampling on and around biological community in the Onnuri Vent Field (OVF), **(B)** copepod *Stygiopontius spinifer* collected from the OVF, and **(C)** bacterial mats on the outer shells of *Bathymodiolus septemdierum* mussels.

consistently higher average $\delta^{15}N_{AA}$ values than source AAs (Gly, Ser, Met, Phe) by 5.5‰ to 12.6‰, with some variation by species. The $\delta^{15}N_{AA}$ offset between trophic AAs and source AAs was higher in *A. marisindica* snail and *I. paucisetus* copepod, with offsets of 12.6 ± 0.6‰ and 11.2 ± 0.5‰, respectively, whereas detritus and shrimp *Alvinocaris* sp. had smaller offsets of 5.5 ± 0.8‰ and 7.6 ± 0.4‰, respectively.

Furthermore, $\delta^{15}N_{Leu}$ and $\delta^{15}N_{Ile}$ values were consistently lower than other trophic AAs in all species and detritus samples, and these values were lower than $\delta^{15}N_{Glu}$ ($\Delta_{Glu\text{-}Leu}$ and $\Delta_{Glu\text{-}Ile}$) by 5.8 ± 3.6‰ and 6.6 ± 3.6‰ on average, respectively. The shrimp *R. kairei*, and copepods *I. paucisetus* and *S. spinifer* had a greater difference in $\Delta_{Glu\text{-}Leu}$ and $\Delta_{Glu\text{-}Ile}$ values than the *B. septemdierum* mussels, ranging from 11.3 ± 1.2‰ to 15.0 ± 1.6‰. Additionally, we found scattered $\delta^{15}N_{Pro}$ values against $\delta^{15}N_{Glu}$ ($\Delta_{Glu\text{-}Pro}$) among vent fauna, with *A. boucheti* snail and *B. septemdierum* mussel having higher $\delta^{15}N_{Pro}$ values than $\delta^{15}N_{Glu}$ values by 9.1 ± 0.6‰ and 7.4 ± 0.9‰, respectively, while a copepod *S. spinifer* and snail *A. marisindica* had ^{15}N-depletion in $\delta^{15}N_{Pro}$ values than $\delta^{15}N_{Glu}$ by 6.0 ± 1.0‰ and 5.5 ± 1.4‰, respectively. The other vent fauna had $\Delta_{Glu\text{-}Pro}$ values in-between.

3.3 Trophic position

The $TP_{Trp\text{-}Phe}$ values calculated using three trophic AAs (Ala, Glu, and Val) have a close alignment with 1:1 line and demonstrate a strong correlation with $TP_{Glu\text{-}Phe}$ values, compared to the other two estimations of $TP_{Trp\text{-}Phe}$ values involving Leu, Ile, and Pro (Figure 3). This discrepancy arises due to the notable variability of the three trophic AAs (Leu, Ile, and Pro) among species. While there may be marginal fluctuations in the absolute $TP_{Trp\text{-}Phe}$ values derived from the three trophic AAs against $TP_{Glu\text{-}Phe}$ values, the overall trend remains consistent and without significant difference. Consequently, our TP dataset will be predicted using $TP_{Glu\text{-}Phe}$ values.

The $TP_{Glu\text{-}Phe}$ ranged from 1.8 ± 0.2 to 3.3 ± 0.1 (Figure 4, Table A2). The two mussel species found in the OVF, *G. vrijenhoeki* and *B. septemdierum*, had different mean TPs, with the former having a value of 1.8 ± 0.2, and the latter having a slightly higher value of 2.3 ± 0.2. The mussel *B. septemdierum* found in the NFB had an intermediate mean value of 2.0 ± 0.4. However, their variation was not statistically significant (ANOVA, $p< 0.109$; Supplementary Material). Among mollusks, *A. marisindica* snail from the OVF had the highest TP of 3.1 ± 0.1, while *A. boucheti* snail from NFB had a slightly lower value of 2.2 ± 0.1, with statistically significant difference (t-test, $p< 0.001$). The two shrimp species found in the OVF had significantly different TPs (*Alvinocaris* sp. = 1.8 ± 0.1; *R. kairei* = 3.3 ± 0.1; *t*-test, $p< 0.001$), while the copepods found at the two vent sites had similarly high TPs of 2.9 ± 0.1 (OVF) and 3.2 ± 0.1 (NFB), with statistical difference (*t*-test, $p< 0.035$). The detritus collected from the OVF had the lowest TP at 1.5 ± 0.1.

TABLE 1 Bulk carbon ($\delta^{13}C$) and nitrogen ($\delta^{15}N$) isotopic compositions of the copepod *Stygiopontius spinifer* and particulate organic matter suction sampled near the biological community as well as bacterial mats on outer shells of *Bathymodiolus septemdierum* mussels (See Figure 1).

Vent	Sample name	$\delta^{13}C$	$\delta^{15}N$
OVF	Copepod *Stygiopontius spinifer*	-12.8 ± 0.1 (2)	10.8 ± 0.1 (2)
OVF	bacterial mats on outer shells of *B. septemdierum*	-27.0 (1)	3.3 ± 0.5 (3)
OVF	Detritus (0.7-38 μm)	-22.7 ± 0.4 (2)	-
OVF	Settled particles (38-100 μm)	-17.5 ± 0.0 (2)	2.8 ± 0.0 (2)

4 Discussion

4.1 Bulk stable isotopic compositions

The $\delta^{15}N$ of muscle tissues in *A. boucheti* snail and *B. septemdierum* mussel from the NFB were higher compared to their gill tissues, which corresponds to the values observed in the OVF, where another snail species (*A. marisindica*), and mussel species *B. septemdierum* and *G. vrijenhoeki* had consistently higher muscle $\delta^{15}N$ values than gill tissues by 1.0 to 2.2‰ (Suh et al., 2022b), indicating a high transfer of nitrogen from the endosymbiotic bacteria to the host. Conversely, the $\delta^{13}C$ values of gill and muscle tissues did not exhibit consistent patterns, having offsets between -0.6 and 0.7‰ in this study and in Suh et al. (2022b). If muscle tissues are ^{13}C-enriched in $\delta^{13}C$ values than gill tissues, it implies that carbon source for hosts is likely originating from endosymbiotic bacteria within the gill tissues. Since we observed both high and low $\delta^{13}C$ values in muscle tissues of host

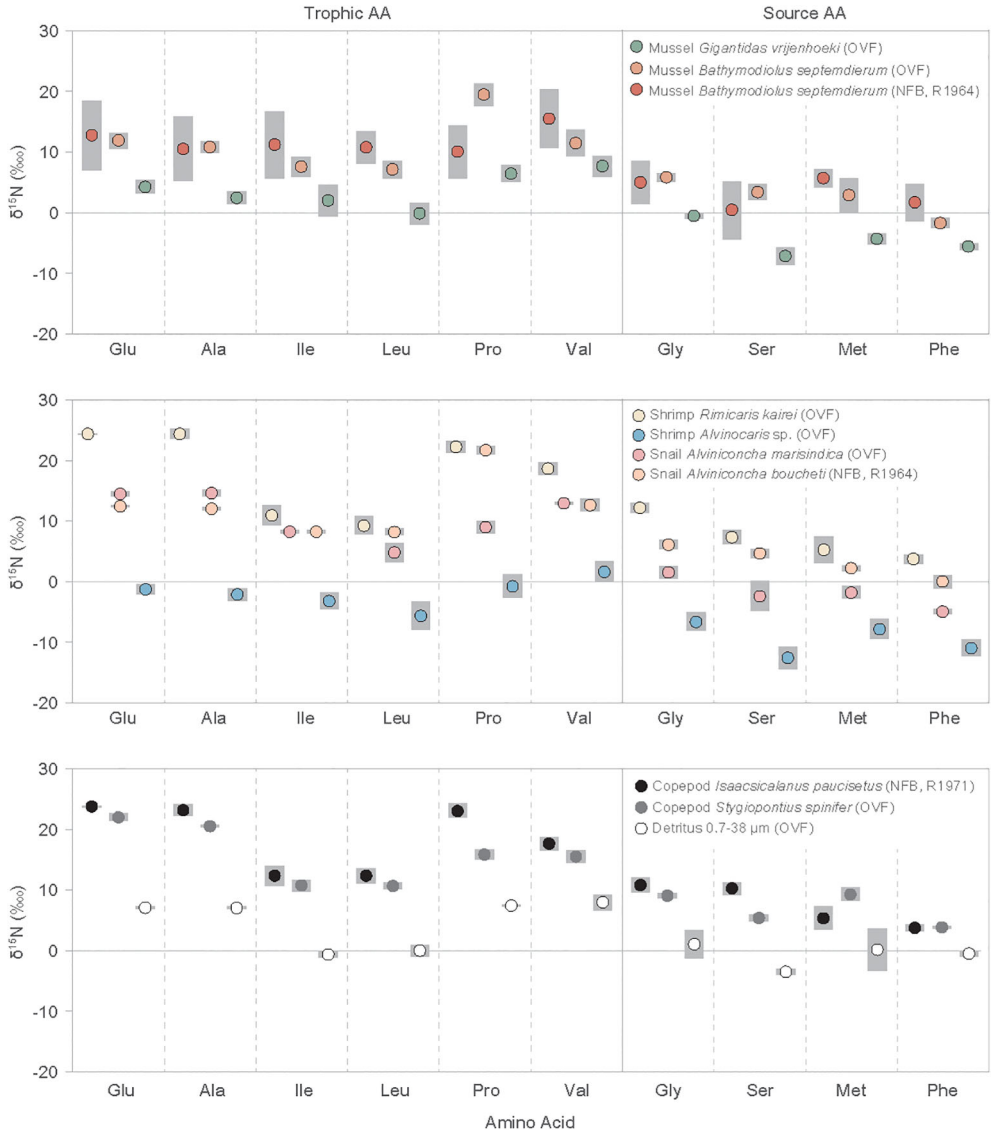

FIGURE 2
Individual amino acid nitrogen isotope values ($\delta^{15}N$) of vent fauna from the Onnuri Vent Field and North Fiji Basin (R1964, R1971) for two or three individual specimens for each species. Gray bars indicate standard deviation. Amino acid abbreviations are: Glu, glutamic acids; Ala, alanine; Ile, isoleucine; Leu, leucine; Pro, proline; Val, valine; Gly, glycine; Ser, serine; Met, methionine; Phe, phenylalanine.

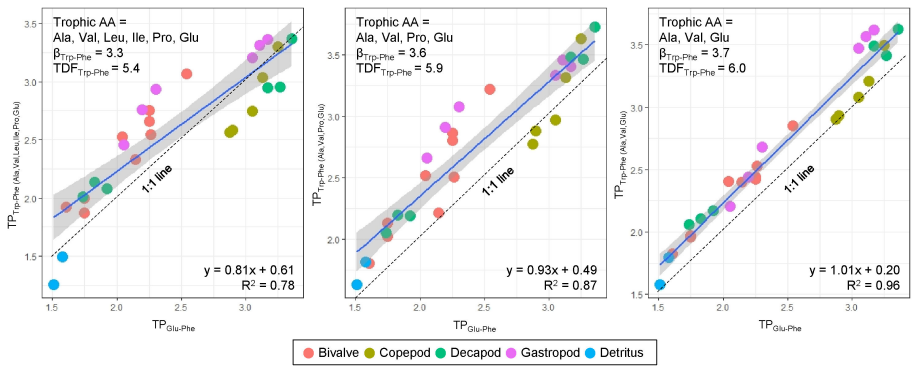

FIGURE 3
Relationship between $TP_{Trp\text{-}Phe}$ and $TP_{Glu\text{-}Phe}$ calculated by three different sets of trophic AAs and corresponding $\beta_{Trp\text{-}Phe}$ and $TDF_{Trp\text{-}Phe}$ values sourced from Chikaraishi et al. (2009). Dotted line denote 1:1 line, where $TP_{Trp\text{-}Phe}$ is equal to $TP_{Glu\text{-}Phe}$.

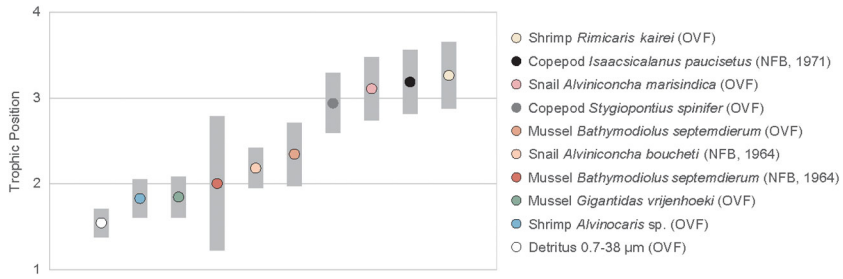

FIGURE 4
Trophic position of vent fauna from the Onnuri Vent Field and North Fiji Basin (R1964, R1971). Gray bars indicate standard deviations calculated using propagated errors (Jarman et al., 2017).

individuals relative to those in gill tissues, hosts have the capacity to access carbon not only from endosymbiotic bacteria but also from ambient materials that they may have filter-fed, including POM, detritus, or free-living bacteria that could be either heterotrophs or autotrophs. The $\delta^{13}C$ and $\delta^{15}N$ values of bacterial mats (Table 1) scraped off the outer shells of mussel *B. septemdierum* suggested that hosts might use them as a carbon source but not for nitrogen metabolism, as indicated by a large $\delta^{15}N$ offset between the mussels and bacterial mats (offset = 13-18‰). This suggests that *B. septemdierum* has different energy sources or different proportions of carbon and nitrogen, as suggested for other vent fauna (Lee and Childress, 1994).

The $\delta^{13}C$ values of snails (*Alviniconcha* spp.) and mussels (*B. septemdierum*) showed only a small variation (~1‰) between the NFB and OVF, indicating that the carbon fixation pathways of the endosymbionts were consistent across both sites despite differing environmental conditions. However, there was a significant difference in $\delta^{15}N$ values of *B. septemdierum* between the two vents, with NFB having a mean $\delta^{15}N$ value of 2.4 ± 0.6‰ (Suh et al., 2022a) and OVF having a mean $\delta^{15}N$ value of -12.1 ± 2.2‰ (Suh et al., 2022b). In contrast, the $\delta^{15}N$ values of *Alviniconcha* spp. did not show such a variation. Low $\delta^{15}N$ values in mussels from different vent locations (Colaço et al., 2002; Naraoka et al., 2008; Van Audenhaege et al., 2019) have frequently been attributed to incomplete utilization of NH_4^+ by bacteria (Rau, 1981b; Van Dover and Fry, 1994; Liao et al., 2014). Seawater samples from both vents were found to have similarly low NH_4^+ concentrations (Table 2), suggesting that endosymbionts may utilize biologically produced ammonium as the main source of nitrogen metabolism instead of using it in seawater. The observation of higher mussel density in the OVF, which has a higher biological production of ammonium, provides further evidence to suggest that lower $\delta^{15}N$ values are associated with biomass (Demopoulos et al., 2019). Another potential factor contributing to ^{15}N-depletion in vent or seep fauna is N_2 fixation, which can occur at sites with methane availability (Dekas et al., 2014), such as OVF. This suggestion can be tested using metagenomic analysis.

The copepod *S. spinifer* from the OVF exhibited the highest $\delta^{15}N$ values (10.8 ± 0.1‰), surpassing those of the shrimp *R. kairei* (7.4 ± 1.8‰; Suh et al., 2022b) and vent crab *Austinograea rodriguezensis* (4.3 ± 2.0‰; Suh et al., 2022b) that are known to be omnivores or carnivores. This copepod species was found residing near an *A. marisindica* snail community and may have obtained some of its carbon energy from the snails, as evidenced by the similar $\delta^{13}C$ values between the two species (*A. marisindica* = -11.4 ± 0.6‰ (Suh et al., 2022b); *S. spinifer* = -12.8‰ (this study)). Moreover, the copepods *S. spinifer* and *R. kairei* utilized isotopically similar sources of carbon and nitrogen, which was supported by the frequent clustering of *R. kairei* around the *A. marisindica* snail community.

4.2 Trophic position of vent fauna

Previous studies on vent fauna from the OVF and NFB (Suh et al., 2022a; Suh et al., 2022b) were unable to accurately determine the TP because of uncertainties in the source nitrogen $\delta^{15}N$ values and isotope fractionation during chemosynthetic metabolism. In this study, we employed the $\delta^{15}N_{AA}$ values to estimate the TP of the vent fauna (Figure 4, Table A2). Our results revealed that the two mussel

TABLE 2 Nutrient concentrations (µM) in the water collected from the Onnuri Vent Field and North Fiji Basin (Suh et al., 2022a).

Site name	Dive number	NH_4 (µM)	NO_2 (µM)	NO_3 (µM)	Reference
OVF	R2196	0.11	0.02	28.50	This study
		0.01	0.02	31.57	
		0.01	0.02	33.14	
		0.02	0.00	34.18	
NFB	R1964	0.95	0.12	8.93	Suh et al., 2022a
		0.98	0.08	6.54	

species from the OVF (*B. septemdierum* and *G. vrijenhoeki*) have slightly different TP (2.3 ± 0.2 and 1.8 ± 0.2, respectively), although the difference was not statistically significant (ANOVA, p = 0.101). Furthermore, the $\delta^{15}N_{Phe}$ values of *B. septemdierum* (-1.7 ± 0.8‰) and *G. vrijenhoeki* (-5.6 ± 0.5‰) suggest that the two species have different nitrogen sources (Figure 5). We posit that this variation could be attributed to differences in their associated symbionts, potentially influencing the nitrogen assimilation. Jang et al. (2020) reported that *B. septemdierum* from the OVF forms a symbiotic relationship with Candidatus *Thioglobus*, while *G. vrijenhoeki* is associated with *Thioglobus*-related Gammaproteobacteria, *Methyloprofundus*-related Gammaproteobacteria, and *Sulfurovum*-related Gammaproteobacteria. Different bacterial diversity in *G. vrijenhoeki* and *B. septemdierum* can lead to different nutrient synthesizing capability. We speculate that the slightly higher TP in *B. septemdierum* could be attributed to energy acquisition not solely from the endosymbionts but also from ambient materials including heterotrophic sources and/or detritus. Conversely, *G. vrijenhoeki* mainly relies on energy sources derived from its symbionts.

Another factor to consider when interpreting trophic relationships between endosymbionts and host animals is the nutrition transfer mechanism that can lead to variations in the TP of the host animal as suggested by Cavanaugh et al. (2006). In one scenario, metabolites synthesized by the autotrophic endosymbionts undergo direct assimilation within the host animal's tissues, resulting in the TP of the host indicative of a primary producer. Another scenario involves the digestion of endosymbiont cells by the host, leading to the TP of the host reflecting that of a consumer, rather than a primary producer. In both scenarios, the host animal's nutrition ultimately comes from the autotrophic endosymbiont. However, the key distinction lies in the processing of the metabolites synthesized by the endosymbiont. These scenarios hold particular significance for herbivores (TP ≈ 2) that mainly rely on endosymbionts for energy and nutrients, as opposed to the omnivores (TP ≥ 2.5) that assimilate heterotrophic or detrital matter as part of their energy sources. Given the available data, the precise mechanism governing the nutrient transfer between endosymbionts and host animals remains challenging to ascertain. However, we note that these underlying factors may partially influence TP variations in herbivores such as the shrimp *Alvinocaris* sp., as well as the mussel species *G. vrijenhoeki* and *B. septemdierum* in this study.

The TP of mussel *B. septemdierum* in the NFB varied greatly from 1.6 to 2.3, suggesting that there is a high degree of intra-species nutritional variability, ranging from consuming symbiont-supported nutrition to ambient sources. This could also be linked to changes in feeding behavior during growth, as smaller mussels (6.7 cm) had a lower TP (1.6) than larger mussels (TPs < 2.0). Previous research has shown that mollusks can shift their diet depending on their body size, although this pattern varies among different locations (Van Dover, 2002; Reid et al., 2016; Reid et al., 2020). Owing to the small sample size (n = 3) and small variation in shell size (~1.3 cm), further investigation is necessary to confirm trophic plasticity in vent mussels. Nevertheless, it is clear that *Bathymodiolus* species in the OVF and NFB feed on both symbiont-derived nutrition and ambient materials (non-symbiont microbes and detritus), with some intra-specific variation.

Several studies have reported on the diversity of symbiotic bacteria and their carbon fixation pathways in *Alviniconcha* snails, but little is known about the contribution of heterotrophic energy to the host and their TP (Suzuki et al., 2005a; Suzuki et al., 2005b; Suzuki et al., 2006; Erickson et al., 2009; Sanders et al., 2013; Beinart et al., 2019; Van Audenhaege et al., 2019; Lee et al., 2021). Based on this study's results, *A. marisindica* in the OVF is an omnivore (TP = 3.1 ± 0.1) that appears to consume detrital sources as part of their diet. The snails (*A. boucheti*) in the NFB, however, is not as omnivorous (TP = 2.2 ± 0.1) as their OVF counterparts (*t*-test, $p < 0.0001$). The reason for this variation between sites may be that OVF has higher biomass, which in turn leads to larger amounts of detritus or heterotrophic OM. This allows organisms to occupy higher TPs because they consume a greater proportion of heterotrophic or detrital OM. We also cannot rule out the variation in gill-associated symbiotic bacteria between the two *Alviniconcha* snail species that may influence their energy acquisition. The predominant symbiotic bacteria of *A. marisindica* snails from the OVF was *Sulfurovum*-related Campylobacteria (Jang et al., 2023), whereas the symbiotic bacteria associated with *A. boucheti* snails was Epsilonproteobacteria genus *Sufurimonas* (unpublished data).

Suh et al. (2022b) classified the shrimp *Alvinocaris* sp. as an omnivorous and opportunistic feeder in the OVF based on its isotopic affinity to omnivores, such as *Munidopsis* sp., and sedimentary OM, which represents the average value of the available food sources in the community. However, in this study, we discovered that *Alvinocaris* sp. is a primary consumer (TP = 1.8 ± 0.1) that mostly relies on symbiotic bacteria for energy (Tokuda et al., 2008; Sun et al., 2016). However, the shrimp *R. kairei* had the highest TP (3.3 ± 0.1) among all the species we analyzed, indicating

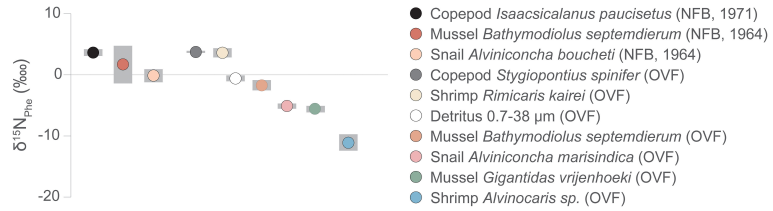

FIGURE 5
$\delta^{15}N_{Phe}$ values, proxy for baseline $\delta^{15}N$ values, of vent fauna from the Onnuri Vent Field and North Fiji Basin (R1964, R1971). Gray bars indicate standard deviation.

that they are scavengers or carnivores. One notable pattern that we observed was that organisms that were often clustered together had similar TPs. For example, the TP of *Alvinocaris* sp. shrimps was similar to that of the *G. vrijenhoeki* mussel (TP = 1.8 ± 0.2), and we collected them from the same locality. The *R. kairei* shrimps were consistently found in hot shimmering areas, and the same was true for *A. marisindica* snails, which are also scavengers with a high TP (3.1 ± 0.1). We speculate that not only the feeding guild but also the energy availability in the microhabitat in which they choose to reside may influence their trophic niche (Versteegh et al., 2022). Variations in symbiotic bacterial community may also have influenced energy assimilation of the host species. Although this study did not analyze symbiotic bacterial diversity in shrimps, a recent study reported a dominance of *Campylobacterota* symbionts in *R. kairei* from the Indian Ocean (Methou et al., 2022). To our knowledge, no reports exist regarding the symbiotic bacterial diversity of *Alvinocaris* sp. from the Indian Ocean. However, it is noteworthy that an *Alvinocaris* congener from Okinawa Trough (*A. longirostris*) exhibited the prevalence of *Sulfurovum* spp. of Epsilonproteobacteria as gill symbionts (Tokuda et al., 2008; Sun et al., 2016).

The copepods had a high TP (2.9 ± 0.1 in OVF, 3.2 ± 0.1 in NFB), contrary to our expectation of them being a link between primary producer and higher TP consumers. The baseline $\delta^{15}N$ values of *S. spinifer* copepods and *R. kairei* shrimps in the OVF were similar (*S. spinifer* $\delta^{15}N_{Phe}$ = 3.9 ± 0.1, *R. kairei* $\delta^{15}N_{Phe}$ = 3.6 ± 0.8), suggesting that they had similar diet sources. Moreover, the copepod *S. spinifer* was found around *Alviniconcha* snails, where *Rimicaris* shrimp was also present, indicating that they utilized detritus or heterotrophic sources available near *Alviniconcha* snail aggregates. The copepod *I. paucisetus* from the diffusive vent in the NFB was also classified as a detritivore or carnivore (TP = 3.2 ± 0.1), and we speculate that they consume detritus derived from the megafaunal community, positioning themselves above the mussels (*B. septemdierum*) and the snails (*A. boucheti*).

4.3 $\delta^{15}N_{AA}$ distribution in vent fauna

Trophic AAs were more enriched in ^{15}N than source AAs in the vent fauna, as observed in all heterotrophs. However, the variation in $\delta^{15}N$ of Leu and Ile compared to that of Glu ($\Delta_{Glu\text{-}Leu}$ and $\Delta_{Glu\text{-}Ile}$, respectively; Figures 6A, B) in some vent fauna differed from that typically observed in heterotrophs from other marine environments. Leu and Ile had lower $\delta^{15}N$ values compared to Glu, with offsets ranging from 1.9‰ to 15.0‰ for $\Delta_{Glu\text{-}Leu}$ and from 1.5‰ to 13.3‰ for $\Delta_{Glu\text{-}Ile}$ on average. This finding is consistent with those of Vokhshoori et al. (2021), that reported low $\delta^{15}N_{Ile}$ and $\delta^{15}N_{Leu}$ values in seep mussels and to a lesser extent, in bacteria and archaea (Yamaguchi et al., 2017). We suggest that this could be due to isotope fractionation during the utilization of Glu to synthesize other AAs as bacteria can utilize Glu to resynthesize other AAs (Davies and Humphrey, 1978; Ponnudurai et al., 2020). The transamination and deamination processes involved in this metabolic pathway preferentially incorporate lighter isotopes, consequently increasing the $\delta^{15}N$ values of the remaining "Glu pool." Furthermore, the high energetic costs associated with the degradation of Ile and Leu in organisms can result in ^{15}N-depletion in these AAs (Akashi and Gojobori, 2002).

Another distinct $\delta^{15}N_{AA}$ pattern observed in vent fauna is the variable offsets of $\delta^{15}N$ values of Pro relative to Glu ($\Delta_{Glu\text{-}Pro}$), which ranged from -9.1 ± 0.6‰ to 6.0 ± 1.0‰ across different species (Figure 6C). Low $\Delta_{Glu\text{-}Pro}$ values were found in *B. septemdierum* mussel (-7.4 ± 0.9‰) and *A. boucheti* snail (-9.1 ± 0.6‰), while high values were recorded in *A. marisindica* snail (5.5 ± 1.4‰) and *S. spinifer* copepod (6.0 ± 1.0‰), with other organisms falling in-between. The underlying mechanism behind such scattered $\delta^{15}N_{AA}$ values among species is still unclear. However, we propose plausible explanations based on the hypotheses presented by Ohkouchi et al. (2017) on scattered $\delta^{15}N_{AA}$ patterns. First, the variability in $\delta^{15}N_{AA}$ values may arise from differences in the quality of OM substrates utilized by microorganisms in the energy biosynthesis process, which are subsequently incorporated into vent fauna (Chikaraishi et al., 2015). Second, it is possible that only selected AAs were microbially resynthesized, resulting from a combination of *de novo* AA synthesis from inorganic nitrogen and salvage incorporation of AAs. This scenario is likely to occur in hydrothermal vents owing to the availability of abundant inorganic nitrogen sources (NO_3^-, NO_2^-, N_2 gas, and NH_4^+) and high biomass concentrations. Third, differences in the metabolic pathways of AAs among species could also contribute to variation in $\delta^{15}N_{AA}$ values. Based on the large variation in bulk $\delta^{15}N$ values observed in vent fauna (-12.1 to 10.8‰ in OVF and -0.8 to 10.4‰ in NFB), it is inferred that multiple nitrogen sources and metabolic pathways are utilized by vent fauna in a single vent field.

4.4 Microbial resynthesis in vent ecosystem

A strong correlation between ΣV and Leu-Ile index has been demonstrated (r^2 = 0.91), suggesting that the low $\delta^{15}N$ in Leu and Ile play a substantial role in the variance within trophic AAs (Figure 7) as was also reported in Vokhshoori et al. (2021). These patterns have been observed in all vent fauna, with some variation in the extent of ^{15}N-depletion in $\delta^{15}N$ of Leu and Ile between species. We found a high ΣV value in detritus (3.4 ± 0.2), indicative of a substantial contribution from reworked OM by heterotrophic bacteria in the OVF. Vent fauna with ΣV values lower than those of detritus, such as *Alvinocaris* sp. and *G. vrijenhoeki*, may have minimal dependence on detrital OM, whereas those with ΣV values similar to or higher than those of detritus likely have mixed dependence on symbiotic and detrital OM. This suggests that host taxa with lower TP rely more on autotrophic chemotrophs for energy, whereas those with higher TPs increasingly rely on heterotrophic OM. However, it is important to note that ΣV index was initially developed in epipelagic detritus that could be presumed to be reworked by heterotrophic bacteria (McCarthy et al., 2007). Although this index can be applied to consumers that rely on bacteria for energy as suggested by Vokhshoori et al. (2021), we take note that metabolism by consumers can potentially influence $\delta^{15}N_{AA}$ distribution and subsequently ΣV values. This aspect necessitates thorough investigation in future studies.

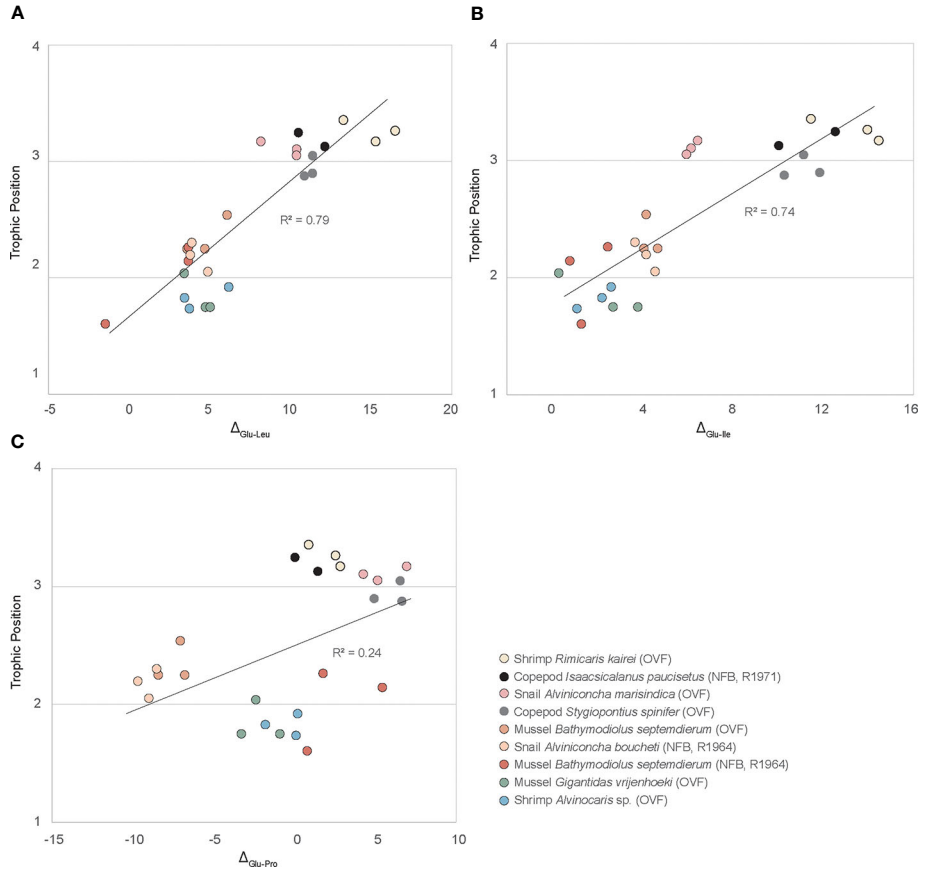

FIGURE 6
Nitrogen isotopic offsets of Leu **(A)**, Ile **(B)**, and Pro **(C)** against Glu versus trophic position of vent fauna from the Onnuri Vent Field and North Fiji Basin (R1964, R1971). $\Delta_{Glu\text{-}Leu} = \delta^{15}N_{Glu} - \delta^{15}N_{Leu}$; $\Delta_{Glu\text{-}Ile} = \delta^{15}N_{Glu} - \delta^{15}N_{Ile}$, $\Delta_{Glu\text{-}Pro} = \delta^{15}N_{Glu} - \delta^{15}N_{Pro}$. Linear regression coefficient (r^2) is indicated for each plot.

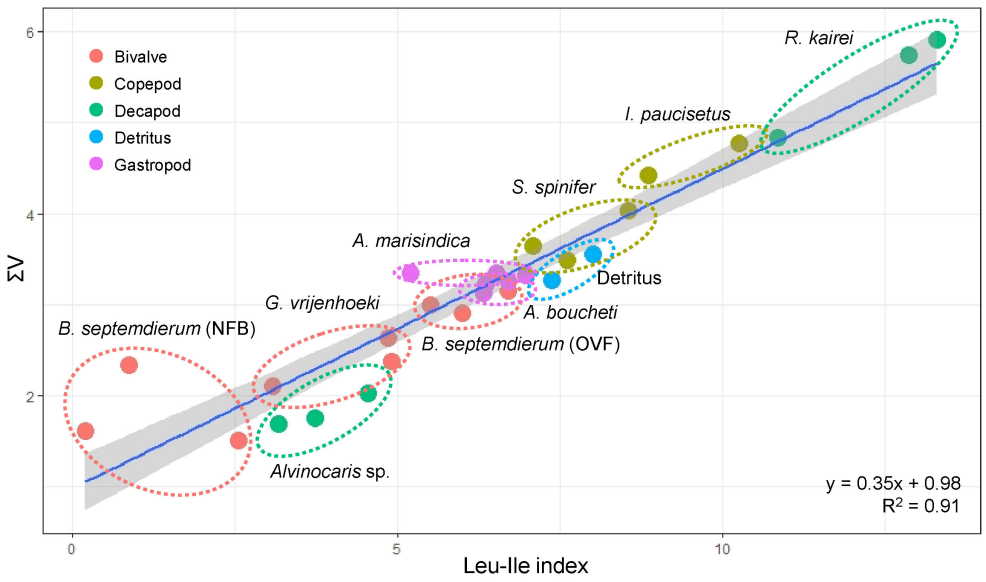

FIGURE 7
Relationship between ΣV and Leu-Ile index in vent fauna from the Onnuri Vent Field (OVF) and North Fiji Basin (NFB).

An increase in the contribution of bacterial AA biomass with increasing TP has been typically observed in littoral environments (Ohkouchi et al., 2017; Vokhshoori et al., 2021), whereas the opposite pattern has been reported in methane seeps (Vokhshoori et al., 2021), where low-TP mussels were suggested to be autotrophic diet feeders and high-TP mussels consumed heterotrophic diets. However, in our study, we did not find such an inverse relationship despite the similarity in primary production processes (i.e., chemosynthesis) between seeps and vents. This discrepancy may be attributed to interspecific variations in the degree of heterotrophic energy contribution. Vokhshoori et al. (2021) looked at ΣV variation across sites for a single species, whereas this study focused on the variation of ΣV between sites for multiple species, at an ecosystem-level. This implies that some symbiont-bearing fauna rely on detritus (i.e., brown food web) as a crucial source of nourishment, with varying degrees of dependence among species. As a result, such effects are reflected in the food web, as demonstrated by the AA-based TP (Steffan et al., 2017). Detritivores are functionally omnivorous, and the omnivorous behavior of hosts suggests that diet flexibility may be a strategy for survival in an ecosystem that is temporally and spatially dynamic.

5 Conclusion

Using $\delta^{15}N_{AA}$ analysis, we determined the TP and extent of heterotrophy in symbiont-bearing taxa found in the hydrothermal vents of the OVF and NFB. These taxa occupied various TPs, ranging from primary consumers to omnivores or carnivores, depending on their feeding guild, environmental conditions, and the species with which they clustered. Our findings showed that the contribution of microbially resynthesized energy increased with TP, particularly in species found in biologically dense ecosystems, such as diffusing vents. This suggests that symbiont-derived energy and detrital or reworked biomass are crucial energy sources for vent fauna. Copepods, which we expected to occupy lower TPs, were found to be carnivores or detritivores, possibly because of trophic inflation caused by the consumption of detrital substrates. Furthermore, we observed low $\delta^{15}N_{Leu}$ and $\delta^{15}N_{Ile}$, and scattered $\delta^{15}N_{Pro}$ values against $\delta^{15}N_{Glu}$ in the vent fauna, with some variation between species. These patterns may serve as indicators of chemosynthetic ecosystems that are distinct from photosynthetic environments. However, it is important to note that $\delta^{15}N_{AA}$ variation in chemosynthetic metabolisms are relatively unexplored compared to photosynthetic systems. Hence, future research efforts should be directed towards unraveling underlying factors contributing to the $\delta^{15}N_{AA}$ patterns in chemosynthetic ecosystem.

Data availability statement

The original contributions presented in the study are included in the article/Supplementary Material. Further inquiries can be directed to the corresponding author.

Ethics statement

The manuscript presents research on animals that do not require ethical approval for their study.

Author contributions

YS, S-JJ, and K-HS contributed to conception and design of the study. M-SK and HC analyzed stable isotopes. YS wrote the first draft of the manuscript. All authors contributed to the article and approved the submitted version.

Funding

The author(s) declare financial support was received for the research, authorship, and/or publication of this article. This research was supported by the Korean Institute of Marine Science and Technology (KIMST) and funded by the Ministry of Oceans and Fisheries (20170411 and 20210634). The isotope analysis was supported by the National Institute of Environmental Research (2022-01-01-072).

Acknowledgments

We are grateful to all crew members and scientists who participated in the exploration cruise and helped with sample collection. We extend our gratitude to Dr. Rho Taekeun and Ms. Son Purena for analyzing nutrient concentrations for this study.

Conflict of interest

The authors declare that the research was conducted in the absence of any commercial or financial relationships that could be construed as a potential conflict of interest.

Publisher's note

Supplementary material

The Supplementary Material for this article can be found online at: https://www.frontiersin.org/articles/10.3389/fmars.2023.1204992/full#supplementary-material

References

Akashi, H., and Gojobori, T. (2002). Metabolic efficiency and amino acid composition in the proteomes of Escherichia coli and Bacillus subtilis. *Proc. Natl. Acad. Sci.* 99, 3695–3700. doi: 10.1073/pnas.062526999

Beinart, R. A., Luo, C., Konstantinidis, K. T., Stewart, F. J., and Girguis, P. R. (2019). The bacterial symbionts of closely related hydrothermal vent snails with distinct geochemical habitats show broad similarity in chemoautotrophic gene content. *Front. Microbiol.* 10. doi: 10.3389/fmicb.2019.01818

Bligh, E. G., and Dyer, W. J. (1959). A rapid method of total lipid extraction and purification. *Can. J. Biochem. Physiol.* 37, 911–917. doi: 10.1139/o59-099

Bourbonnais, A., Lehmann, M. F., Butterfield, D. A., and Juniper, S. K. (2012). Subseafloor nitrogen transformations in diffuse hydrothermal vent fluids of the Juan de Fuca Ridge evidenced by the isotopic composition of nitrate and ammonium. *Geochemistry Geophysics Geosystems* 13, 4661-4678. doi: 10.1029/2011GC003863

Cavanaugh, C. M., McKiness, Z. P., Newton, I. L., and Stewart, F. J. (2006). Marine chemosynthetic symbioses. *prokaryotes* 1, 475–507. doi: 10.1007/0-387-30741-9_18

Chang, N.-N., Lin, L.-H., Tu, T.-H., Jeng, M.-S., Chikaraishi, Y., and Wang, P.-L. (2018). Trophic structure and energy flow in a shallow-water hydrothermal vent: Insights from a stable isotope approach. *PLoS One* 13, e0204753. doi: 10.1371/journal.pone.0204753

Charoenpong, C. C. N. (2019). The production and fate of nitrogen species in deep-sea hydrothermal environments.

Chikaraishi, Y., Ogawa, N. O., Kashiyama, Y., Takano, Y., Suga, H., Tomitani, A., et al. (2009). Determination of aquatic food-web structure based on compound-specific nitrogen isotopic composition of amino acids. *Limnology Oceanography: Methods* 7, 740–750. doi: 10.4319/lom.2009.7.740

Chikaraishi, Y., Steffan, S. A., Takano, Y., and Ohkouchi, N. (2015). Diet quality influences isotopic discrimination among amino acids in an aquatic vertebrate. *Ecol. Evol.* 5, 2048–2059. doi: 10.1002/ece3.1491

Childress, J., and Fisher, C. R. (1992). The biology of hydrothermal vent animals: Physiology, biochemistry, and autotrophic symbioses. *Oceanography Mar. Biology: Annu. Rev.* 30, 337–441.

Colaço, A., Dehairs, F., and Desbruyères, D. (2002). Nutritional relations of deep-sea hydrothermal fields at the Mid-Atlantic Ridge: A stable isotope approach. *Deep-Sea Res. Part I: Oceanographic Res. Papers* 49, 395–412. doi: 10.1016/S0967-0637(01)00060-7

Corliss, J. B., Dymond, J., Gordon, L. I., Edmond, J. M., von Herzen, R. P., Ballard, R. D., et al. (1979). Submarine thermal springs on the galápagos rift. *Science* 203, 1073–1083. doi: 10.1126/science.203.4385.1073

Davies, D. D., and Humphrey, T. J. (1978). Amino Acid recycling in relation to protein turnover. *Plant Physiol.* 61, 54–58. doi: 10.1104/pp.61.1.54

Dekas, A. E., Chadwick, G. L., Bowles, M. W., Joye, S. B., and Orphan, V. J. (2014). Spatial distribution of nitrogen fixation in methane seep sediment and the role of the ANME archaea. *Environ. Microbiol.* 16, 3012–3029. doi: 10.1111/1462-2920.12247

Demopoulos, A. W. J., McClain-Counts, J. P., Bourque, J. R., Prouty, N. G., Smith, B. J., Brooke, S., et al. (2019). Examination of Bathymodiolus childressi nutritional sources, isotopic niches, and food-web linkages at two seeps in the US Atlantic margin using stable isotope analysis and mixing models. *Deep Sea Res. Part I: Oceanographic Res. Papers* 148, 53–66. doi: 10.1016/j.dsr.2019.04.002

Erickson, K., Macko, S., and Van Dover, C. (2009). Evidence for a chemoautotrophically based food web at inactive hydrothermal vents (Manus Basin). *Deep Sea Res. Part II: Topical Stud. Oceanography* 56, 1577–1585. doi: 10.1016/j.dsr2.2009.05.002

Fisher, C. R., Childress, J. J., Arp, A. J., Brooks, J. M., Distel, D., Favuzzi, J. A., et al. (1988). Microhabitat variation in the hydrothermal vent mussel, Bathymodiolus thermophilus, at the Rose Garden vent on the Galapagos Rift. *Deep Sea Res. Part A Oceanographic Res. Papers* 35, 1769–1791. doi: 10.1016/0198-0149(88)90049-0

Fisher, C. R., Childress, J. J., Macko, S. A., and Brooks, J. M. (1994). Nutritional interactions in Galapagos rift hydrothermal vent communities: Inferences from stable carbon and nitrogen isotope analyses. *Mar. Ecol. Prog. Ser.* 103, 45–56. doi: 10.3354/meps103045

Fry, B. (2006). *Stable isotope ecology* (New Yokr, NY: Springer).

Jang, S.-J., Cho, S.-Y., Li, C., Zhou, Y., Wang, H., Sun, J., et al. (2023). Geographical subdivision of Alviniconcha snail populations in the Indian Ocean hydrothermal vent regions. *Front. Mar. Sci.* 10. doi: 10.3389/fmars.2023.1139190

Jang, S.-J., Ho, P.-T., Jun, S.-Y., Kim, D., and Won, Y.-J. (2020). A newly discovered Gigantidas bivalve mussel from the Onnuri Vent Field in the northern Central Indian Ridge. *Deep Sea Res. Part I: Oceanographic Res. Papers* 161, 103299. doi: 10.1016/j.dsr.2020.103299

Jannasch, H. W., and Wirsen, C. O. (1979). Chemosynthetic primary production at East Pacific sea floor spreading centers. *Bioscience* 29, 592–598. doi: 10.2307/1307765

Jarman, C. L., Larsen, T., Hunt, T., Lipo, C., Solsvik, R., Wallsgrove, N., et al. (2017). Diet of the prehistoric population of Rapa Nui (Easter Island, Chile) shows environmental adaptation and resilience. *Am. J. Phys. Anthropology* 164, 343–361. doi: 10.1002/ajpa.23273

Kennicutt, M. C., Burke, R. A., MacDonald, I. R., Brooks, J. M., Denoux, G. J., and Macko, S. A. (1992). Stable isotope partitioning in seep and vent organisms: chemical and ecological significance. *Chem. Geology: Isotope Geosci. section* 101, 293–310. doi: 10.1016/0009-2541(92)90009-T

Kim, J., Son, S.-K., Kim, D., Pak, S.-J., Yu, O. H., Walker, S. L., et al. (2020). Discovery of active hydrothermal vent fields along the central Indian ridge, 8–12°S. *Geochemistry Geophysics Geosystems* 21, e2020GC009058. doi: 10.1029/2020gc009058

Kim, M.-S., Lee, W.-S., Suresh Kumar, K., Shin, K.-H., Robarge, W., Kim, M., et al. (2016). Effects of HCl pretreatment, drying, and storage on the stable isotope ratios of soil and sediment samples. *Rapid Commun. Mass Spectrometry* 30, 1567–1575. doi: 10.1002/rcm.7600

Lee, J., Kim, D., and Kim, I.-H. (2020). Copepoda (Siphonostomatoida: Dirivultidae) from hydrothermal vent fields on the central Indian Ridge, Indian Ocean. *Zootaxa* 4759, 301–337-301–337. doi: 10.11646/zootaxa.4759.3.1

Lee, R. W., and Childress, J. J. (1994). Assimilation of inorganic nitrogen by marine invertebrates and their chemoautotrophic and methanotrophic symbionts. *Appl. Environ. Microbiol.* 60, 1852–1858. doi: 10.1128/AEM.60.6.1852-1858.1994

Lee, W.-K., Juniper, S. K., Perez, M., Ju, S.-J., and Kim, S.-J. (2021). Diversity and characterization of bacterial communities of five co-occurring species at a hydrothermal vent on the Tonga Arc. *Ecol. Evol.* 11, 4481–4493. doi: 10.1002/ece3.7343

Liao, L., Wankel, S. D., Wu, M., Cavanaugh, C. M., and Girguis, P. R. (2014). Characterizing the plasticity of nitrogen metabolism by the host and symbionts of the hydrothermal vent chemoautotrophic symbioses Ridgeia piscesae. *Mol. Ecol.* 23, 1544–1557. doi: 10.1111/mec.12460

Lonsdale, P. (1977). Clustering of suspension-feeding macrobenthos near abyssal hydrothermal vents at oceanic spreading centers. *Deep Sea Res.* 24, 857–863. doi: 10.1016/0146-6291(77)90478-7

McCarthy, M. D., Benner, R., Lee, C., and Fogel, M. L. (2007). Amino acid nitrogen isotopic fractionation patterns as indicators of heterotrophy in plankton, particulate, and dissolved organic matter. *Geochimica Cosmochimica Acta* 71, 4727–4744. doi: 10.1016/j.gca.2007.06.061

McMahon, K., and McCarthy, M. (2016). Embracing variability in amino acid δ15N fractionation: Mechanisms, implications, and applications for trophic ecology. *Ecosphere* 7, e01511. doi: 10.1002/ecs2.1511

Methou, P., Hikosaka, M., Chen, C., Watanabe, H. K., Miyamoto, N., Makita, H., et al. (2022). Symbiont community composition in rimicaris kairei shrimps from Indian ocean vents with notes on mineralogy. *Appl. Environ. Microbiol.* 88, e0018522. doi: 10.1128/aem.00185-22

Naraoka, H., Naito, T., Yamanaka, T., Tsunogai, U., and Fujikura, K. (2008). A multi-isotope study of deep-sea mussels at three different hydrothermal vent sites in the northwestern Pacific. *Chem. Geology* 255, 25–32. doi: 10.1016/j.chemgeo.2008.05.015

Ohkouchi, N., Chikaraishi, Y., Close, H. G., Fry, B., Larsen, T., Madigan, D. J., et al. (2017). Advances in the application of amino acid nitrogen isotopic analysis in ecological and biogeochemical studies. *Organic Geochemistry* 113, 150–174. doi: 10.1016/j.orggeochem.2017.07.009

Park, C., Lee, W.-K., Kim, S.-J., and Ju, S.-J. (2020). DNA barcoding of isaacsicalanus paucisetus (Copepoda: calanoida: spinocalanidae) from the hydrothermal vent in the North Fiji Basin, Southwestern Pacific Ocean. *Anim. Systematics Evol. Diversity* 36, 182–184. doi: 10.5635/ASED.2020.36.2.013

Polz, M. F., Robinson, J. J., Cavanaugh, C. M., and Van Dover, C. L. (1998). Trophic ecology of massive shrimp aggregations at a Mid-Atlantic Ridge hydrothermal vent site. *Limnology Oceanography* 43, 1631–1638. doi: 10.4319/lo.1998.43.7.1631

Pond, D. W., Dixon, D. R., Bell, M. V., Fallick, A. E., and Sargent, J. R. (1997). Occurrence of 16: 2 (n-4) and 18: 2 (n-4) fatty acids in the lipids of the hydrothermal vent shrimps Rimicaris exoculata and Alvinocaris markensis: nutritional and trophic implications. *Mar. Ecol. Prog. Ser.* 156, 167–174. doi: 10.3354/meps156167

Ponnudurai, R., Heiden, S. E., Sayavedra, L., Hinzke, T., Kleiner, M., Hentschker, C., et al. (2020). Comparative proteomics of related symbiotic mussel species reveals high variability of host–symbiont interactions. *ISME J.* 14, 649–656. doi: 10.1038/s41396-019-0517-6

Portail, M., Brandily, C., Cathalot, C., Colaço, A., Gélinas, Y., Husson, B., et al. (2018). Food-web complexity across hydrothermal vents on the Azores triple junction. *Deep Sea Res. Part I: Oceanographic Res. Papers* 131, 101–120. doi: 10.1016/j.dsr.2017.11.010

Rau, G. H. (1981a). Hydrothermal vent clam and tube worm 13C/12C: Further evidence of nonphotosynthetic food sources. *Science* 213, 338–340. doi: 10.1126/science.213.4505.338

Rau, G. H. (1981b). Low 15N/14N in hydrothermal vent animals: ecological implications. *Nature* 289, 484–485. doi: 10.1038/289484a0

Rau, G. H., and Hedges, J. I. (1979). Carbon-13 depletion in a hydrothermal vent mussel: suggestion of a chemosynthetic food source. *Science* 203, 648–649. doi: 10.1126/science.203.4381.648

Reid, W. D. K., Sweeting, C. J., Wigham, B. D., McGill, R. A. R., and Polunin, N. V. C. (2016). Isotopic niche variability in macroconsumers of the East Scotia Ridge (Southern Ocean) hydrothermal vents: What more can we learn from an ellipse? *Mar. Ecol. Prog. Ser.* 542, 13–24. doi: 10.3354/meps11571

Reid, W. D. K., Wigham, B. D., Marsh, L., Weston, J. N. J., Zhu, Y., and Copley, J. T. (2020). Trophodynamics at the Longqi hydrothermal vent field and comparison with the East Scotia and Central Indian Ridges. *Mar. Biol.* 167, 141. doi: 10.1007/s00227-020-03755-1

Salcedo, D. L., Soto, L. A., and Paduan, J. B. (2021). Trophic interactions among the macrofauna of the deep-sea hydrothermal vents of Alarcón Rise, Southern Gulf of California. *Deep Sea Res. Part I: Oceanographic Res. Papers* 176, 103609. doi: 10.1016/j.dsr.2021.103609

Sanders, J. G., Beinart, R. A., Stewart, F. J., Delong, E. F., and Girguis, P. R. (2013). Metatranscriptomics reveal differences in *in situ* energy and nitrogen metabolism among hydrothermal vent snail symbionts. *ISME J.* 7, 1556–1567. doi: 10.1038/ismej.2013.45

Steffan, S. A., Chikaraishi, Y., Dharampal, P. S., Pauli, J. N., Guédot, C., and Ohkouchi, N. (2017). Unpacking brown food-webs: Animal trophic identity reflects rampant microbivory. *Ecol. Evol.* 7, 3532–3541. doi: 10.1002/ece3.2951

Suh, Y. J., Kim, M.-S., Kim, S.-J., Kim, D., and Ju, S.-J. (2022b). Carbon sources and trophic interactions of vent fauna in the Onnuri Vent Field, Indian Ocean, inferred from stable isotopes. *Deep Sea Res. Part I: Oceanographic Res. Papers* 182, 103683. doi: 10.1016/j.dsr.2021.103683

Suh, Y., Kim, M.-S., Lee, W. K., Yoon, H., Moon, I., Jung, J., et al. (2022a). Niche partitioning of hydrothermal vent fauna in the North Fiji Basin, Southwest Pacific inferred from stable isotopes. *Mar. Biol.* 169, 149. doi: 10.1007/s00227-022-04129-5

Sun, Q.-l., Zeng, Z.-g., Chen, S., and Sun, L. (2016). First comparative analysis of the community structures and carbon metabolic pathways of the bacteria associated with alvinocaris longirostris in a hydrothermal vent of okinawa trough. *PLoS One* 11, e0154359. doi: 10.1371/journal.pone.0154359

Suzuki, Y., Kojima, S., Sasaki, T., Suzuki, M., Utsumi, T., Watanabe, H., et al. (2006). Host-symbiont relationships in hydrothermal vent gastropods of the genus Alviniconcha from the Southwest Pacific. *Appl. Environ. Microbiol.* 72, 1388–1393. doi: 10.1128/aem.72.2.1388-1393.2006

Suzuki, Y., Sasaki, T., Suzuki, M., Nogi, Y., Miwa, T., Takai, K., et al. (2005a). Novel chemoautotrophic endosymbiosis between a member of the Epsilonproteobacteria and the hydrothermal-vent gastropod Alviniconcha aff. hessleri (Gastropoda: Provannidae) from the Indian Ocean. *Appl. Environ. Microbiol.* 71, 5440–5450. doi: 10.1128/aem.71.9.5440-5450.2005

Suzuki, Y., Sasaki, T., Suzuki, M., Tsuchida, S., Nealson, K. H., and Horikoshi, K. (2005b). Molecular phylogenetic and isotopic evidence of two lineages of chemoautotrophic endosymbionts distinct at the subdivision level harbored in one host-animal type: the genus Alviniconcha (Gastropoda: Provannidae). *FEMS Microbiol. Lett.* 249, 105–112. doi: 10.1016/j.femsle.2005.06.023

Tokuda, G., Yamada, A., Nakano, K., Arita, N. O., and Yamasaki, H. (2008). Colonization of Sulfurovum sp. on the gill surfaces of Alvinocaris longirostris, a deep-sea hydrothermal vent shrimp. *Mar. Ecol.* 29, 106–114. doi: 10.1111/j.1439-0485.2007.00211.x

Van Audenhaege, L., Fariñas-Bermejo, A., Schultz, T., and Lee Van Dover, C. (2019). An environmental baseline for food webs at deep-sea hydrothermal vents in Manus Basin (Papua New Guinea). *Deep Sea Res. Part I: Oceanographic Res. Papers* 148, 88–99. doi: 10.1016/j.dsr.2019.04.018

Van Dover, C. (2002). Trophic relationships among invertebrates at the Kairei hydrothermal vent field (Central Indian Ridge). *Mar. Biol.* 141, 761–772. doi: 10.1007/s00227-002-0865-y

Van Dover, C. L., and Fry, B. (1994). Microorganisms as food resources at deep-sea hydrothermal vents. *Limnology Oceanography* 39, 51–57. doi: 10.4319/lo.1994.39.1.0051

Versteegh, E. A. A., Van Dover, C. L., Van Audenhaege, L., and Coleman, M. (2022). Multiple nutritional strategies of hydrothermal vent shrimp (Rimicaris hybisae) assemblages at the Mid-Cayman Rise. *Deep Sea Res. Part I: Oceanographic Res. Papers* 192, 103915. doi: 10.1016/j.dsr.2022.103915

Vokhshoori, N. L., McCarthy, M. D., Close, H. G., Demopoulos, A. W. J., and Prouty, N. G. (2021). New geochemical tools for investigating resource and energy functions at deep-sea cold seeps using amino acid δ15N in chemosymbiotic mussels (Bathymodiolus childressi). *Geobiology* 19, 601–617. doi: 10.1111/gbi.12458

Wang, X., Li, C., Wang, M., and Zheng, P. (2018). Stable isotope signatures and nutritional sources of some dominant species from the PACManus hydrothermal area and the Desmos caldera. *PLoS One* 13, e0208887. doi: 10.1371/journal.pone.0208887

Wang, F., Wu, Y., and Feng, D. (2022). Different nitrogen sources fuel symbiotic mussels at cold seeps. *Front. Mar. Sci.* 9. doi: 10.3389/fmars.2022.869226

Yamaguchi, Y., Chikaraishi, Y., Takano, Y., Ogawa, N., Imachi, H., Yokoyama, Y., et al. (2017). Fractionation of nitrogen isotopes during amino acid metabolism in heterotrophic and chemolithoautotrophic microbes across Eukarya, Bacteria, and Archaea: Effects of nitrogen sources and metabolic pathways. *Organic Geochemistry* 111, 101-112. doi: 10.1016/j.orggeochem.2017.04.004